JOURNAL OF COMPUTATIONAL PHYSICS 25, 71–93 (1977)

The Solution of Poisson's Equation for Isolated Source Distributions

R. A. JAMES

University of Manchester, Department of Astronomy, Manchester, England

Received April 30, 1976; revised October 14, 1976

The potential due to an isolated finite distribution of sources satisfies a zero condition at infinity in three dimensions, or a logarithmic condition in two. It may be evaluated on a finite mesh by means of a fast potential solver for the mesh, combined with a procedure for the potential on the mesh boundary. This paper describes a way of calculating the boundary potential by finding a set of correction charges on the boundary only, and convolving them with a suitable Green's function. The advantage over the usual convolution techniques is that mesh doubling is needed for boundary points only. The process is equivalent to convolving the source distribution with the Green's function, but requires less storage and computer time. The choice of Green's function is constrained by the finite difference approximation used for the Laplace operator.

1. INTRODUCTION

Fast Fourier transform techniques have proved to be a powerful tool in the solution of the Poisson equation on rectangular meshes. We express the equation in discrete form by means of a suitable finite difference approximation to the Laplace operator. A Fourier transformation parallel to any mesh axis diagonalizes the discrete equation as far as that axis is concerned. Transformation parallel to each of the mesh axes diagonalizes the equation completely. Thus one practical method of solution is to perform such a Fourier analysis, to solve for the potential in transform space, and then perform an inverse analysis (or synthesis). Hockney [9] gives a review of this and of other techniques, and discusses the advantages of omitting the last Fourier transform stage and solving the final set of equations directly.

The major restriction of this method arises from the boundary conditions. The only cases which are easy to handle are those where (i) the potential is known on the boundary, (ii) the field is known on the boundary, or (iii) the potential and charge distributions are periodic. These cases correspond to the sine, cosine, and periodic Fourier transforms, respectively. Boundary conditions may be mixed, provided that the same type of condition applies to both members of any pair of parallel boundaries.

In all cases the operation count for the procedure above has leading term $5N \log_2 N$ for a mesh of N points. The count may be reduced by using Hockney's FACR algorithms [9]. It is sometimes claimed that problems with prescribed boundary potential or field require twice this number of operations. Hockney notes that this need not be

ISSN 0021-9991

the case, and Ziegler [15] has given a process for the cosine transform with essentially the same operation count as the processes generally used for the periodic transform. A similar process may be constructed for the sine transform.

Another important problem is that of the "free space" potential due to a finite charge distribution. This satisfies a zero condition at infinity for three-dimensional problems, or a logarithmic condition in two dimensions. We refer to this as the case of an isolated charge distribution. To apply Fast Fourier Transform (FFT) techniques, we must determine the potential on the boundary of a finite mesh containing the source charges. Hockney [8] has approached this problem by using a low-order expansion in a two-dimensional case. The technique has been extended to three dimensions [14]. It is however approximate, and most workers use instead a convolution procedure based on the FFT. The latter technique is described in Ref. [9]. It involves using twice the storage required for the original mesh, and even to achieve this figure requires some ingenuity [10, 11]. The number of operations needed can be shown to amount to 14/3 times that for the simpler cases above.

This paper describes a way of reducing the problem for an isolated charge distribution to that for known potential on the mesh boundary. Von Hagenow and Lackner [7] have pointed out that we may split the required potential into two components:

(1) The potential ϕ obtained from the charges at interior points of the mesh, together with a zero potential on the mesh boundary.

(2) The potential ψ arising from a set of correction charges on the mesh boundary only. These charges may be determined once we know ϕ, and they include the prescribed boundary charges. Von Hagenow and Lackner have applied this technique successfully to two-dimensional problems. It is related to the imbedding method of Buzbee *et al.* [4]. We extend it here to the three-dimensional case.

In Section 2 of this paper we give an outline of the boundary correction charge procedure. The calculation of the correction charges, and of the potentials ϕ and ψ at interior points of the mesh, is considered in Section 3. Section 4 describes the calculation of the boundary values of ψ and Section 5 that of the Green's functions. The final section summarizes the performance of the process. For the sake of clarity, Sections 3 and 5 work mainly in terms of a simple finite difference approximation to the Laplace operator. More elaborate and accurate representations are given in Appendix A, and information about the corresponding Green's functions in Appendix B. Appendix C lists conversion formulas appropriate to the various finite difference Laplace operators used.

2. The Boundary Correction Charge Technique

We denote the (possibly unequal) mesh intervals by h_1, h_2, h_3 and assume that the source charges are restricted to a rectangular region $\mathscr{R}$ of the mesh. We take our origin at a mesh point at one corner of this region, so that the general mesh point has coordi-

nates (rh_1, sh_2, th_3), r, s, t being integers. The simplest finite difference representation available for the Poisson equation

$$\nabla^2\phi = -4\pi\rho \tag{2.1}$$

is

$$(h_1^{-2}\delta_1^{\,2} + h_2^{-2}\delta_2^{\,2} + h_3^{-2}\delta_3^{\,2})\,\phi_{rst} = -4\pi\rho_{rst} \tag{2.2}$$

where

$$\phi_{rst} = \phi(rh_1, sh_2, th_3), \tag{2.3}$$

$$\rho_{rst} = \rho(rh_1, sh_2, th_3), \tag{2.4}$$

and the suffix attached to the operator δ indicates the direction in which we are differencing.

Our first step is to solve for the potential ϕ_{rst} defined by the prescribed charges inside $\mathscr{R}$, together with a zero potential on the boundary of $\mathscr{R}$. For the moment we ignore the prescribed charges on the boundary. Outside $\mathscr{R}$ we set ϕ_{rst}, ρ_{rst} to zero. With this extension to the infinite region, ϕ_{rst} is clearly a free space potential generated by a distribution of source charges confined to $\mathscr{R}$. As ϕ_{rst} satisfies Eq. (2.2) inside $\mathscr{R}$, this distribution is just the prescribed distribution there. On the boundary of $\mathscr{R}$ however, we may apply Eq. (2.2) to find a set of screening charges which are not usually equal to the prescribed charges. Thus the prescribed source distribution may be thought of as the sum of the distribution generating ϕ, and of a set of correction charges on the boundary of $\mathscr{R}$. Clearly the potential ψ arising from these correction charges is the supplement which we must add to ϕ to obtain the free space potential we require.

To determine ψ, we find first its values on the mesh boundary. We calculate these values by a convolution procedure based on the FFT. As only boundary charges and potentials are involved, this is a much smaller calculation than a full convolution on the mesh. We extend ψ into the interior of $\mathscr{R}$ by means of the standard equivalent charge technique [9].

The system of screening charges is, of course, the discrete analog of the charges which appear on the surface of an earthed conductor enclosing a continuous charge distribution. We note that other finite difference approximations to Eq. (2.1) may introduce additional layers of screening charges. For example, if we include the fourth difference term

$$-\tfrac{1}{12}(h_1^{-2}\delta_1^{\,4} + h_2^{-2}\delta_2^{\,4} + h_3^{-2}\delta_3^{\,4})\phi_{rst} \tag{2.5}$$

on the left-hand side of Eq. (2.2), we require screening charges on the planes adjacent to the boundary planes as well. These additional charges would greatly complicate the boundary calculation. We may avoid their appearance by "throwing back" the fourth difference terms of expression (2.5) to terms of the form $\delta_1^{\,2}\,\delta_2^{\,2}\,\phi_{rst}$ and so on [6, 13]. For the special case of a symmetric mesh geometry,

$$h_1 = h_2 = h_3 \tag{2.6}$$

the sixth difference terms also may be thrown back. The resulting formulas are given in Appendix A. Thus we have a choice of two finite difference operators for the general case, or three for the case of Eq. (2.6). All these operators generate a single layer of correction charges on the boundary of $\mathscr{R}$, and may be treated by the methods of this paper.

The boundary calculation is the main overhead of the method additional to that for the case of prescribed boundary potential. The overhead is reasonable as regards operation count, and small as regards storage requirements. In practice, unless the mesh contains very few points, we find that less than half the total computing time is needed for boundary values of ψ, and the store required is only slightly greater than that for the original data. Thus we require about 30 % of the computing time and 50 % of the core needed for the ordinary convolution technique.

The price we pay for this gain is that the Green's function we use in the boundary calculation must arise from inverting the finite difference approximation for the Laplace operator. ψ satisfies the Laplace equation (in the discrete approximation) at all points off the mesh boundary. Since ψ is just a weighted sum of contributions from the correction charges, each individual contribution must satisfy this equation at all mesh points other than that where its source is located. Buneman [2, 3] has given inversions for various two-dimensional forms of the Laplace operator. A convenient but less elegant technique for two and three-dimensional cases is given in Section 5 of this paper.

None of our forms for the discrete equation is satisfied exactly by the Newtonian potential $1/R$, R being the geometric distance from the source. Our Green's functions are thus approximations to $1/R$. The quality of an approximation depends on the accuracy of the corresponding discrete Laplace operator.

3. Calculation of Interior Potentials and Boundary Correction Charges

The current version of the method uses the "poor man's Poisson solver" of Boris and Roberts [1] to determine interior potentials. The procedure is simple, but less efficient than Hockney's FACR algorithms. It would be possible to incorporate FACR procedures in the method, but so far this has not been done.

In this section, for the sake of clarity, we consider only the case where r, s, t have the same range $(0, N)$, and we also restrict ourselves to the simple finite difference representation of Eq. (2.2). These are not restrictions in the method or in the current software.

If x_{rst} is any quantity defined on the mesh, we write

$$x^{\alpha\beta\gamma} = \sum_{r,s,t=1}^{N-1} x_{rst} \sin\frac{\pi r\alpha}{N} \sin\frac{\pi s\beta}{N} \sin\frac{\pi t\gamma}{N}. \tag{3.1}$$

We write Eq. (2.2) as

$$\mathscr{L}_1 \phi_{rst} = (w_1 \delta_1^2 + w_2 \delta_2^2 + w_3 \delta_3^2)\, \phi_{rst} = -q_{rst} \tag{3.2}$$

where

$$w_i = h_i^{-2}/2(h_1^{-2} + h_2^{-2} + h_3^{-2}) \tag{3.3}$$

and

$$q_{rst} = 2\pi\rho_{rst}/(h_1^{-2} + h_2^{-2} + h_3^{-2}). \tag{3.4}$$

A sine transformation, as in Eq. (3.1), reduces Eq. (3.2) to the form

$$\phi^{\alpha\beta\gamma} = q^{\alpha\beta\gamma}/C^{\alpha\beta\gamma} \tag{3.5}$$

where

$$C^{\alpha\beta\gamma} = 2w_1\left(1 - \cos\frac{\pi\alpha}{N}\right) + 2w_2\left(1 - \cos\frac{\pi\beta}{N}\right) + 2w_3\left(1 - \cos\frac{\pi\gamma}{N}\right). \tag{3.6}$$

To calculate the screening charges on (for example) the boundary $r = 0$, we apply Eq. (3.2) at the point $(0, s, t)$. Of the potentials involved on the left-hand side, only those on the plane $r = 1$ are nonzero, so we may write

$$Q'_{0st} = -(\mathscr{L}_1\phi)_{0st} = -w_1\phi_{1st}\,. \tag{3.7}$$

The symbol Q' has been used in this last equation to distinguish the screening charges from the prescribed charges q. The correction charges are then given by

$$Q_{0st} = q_{0st} - Q'_{0st}\,. \tag{3.8}$$

We could calculate the potentials ϕ_{1st}, together with the other boundary adjacent potentials required, by synthesizing $\phi^{\alpha\beta\gamma}$. This procedure is needlessly costly, however. Consider as an example the potentials ϕ_{1st}, $\phi_{N-1,st}$ and denote their transforms in directions 2 and 3 by

$$\phi_1^{\cdot\beta\gamma} = \sum_{s,t=1}^{N-1} \phi_{1st} \sin\frac{\pi s\beta}{N} \sin\frac{\pi t\gamma}{N} \tag{3.9}$$

and

$$\phi_{N-1}^{\cdot\beta\gamma} = \sum_{s,t=1}^{N-1} \phi_{N-1,st} \sin\frac{\pi s\beta}{N} \sin\frac{\pi t\gamma}{N}\,. \tag{3.10}$$

These transforms may be calculated from the triple transform $\phi^{\alpha\beta\gamma}$ by the expressions

$$\phi_1^{\cdot\beta\gamma} = \sum_{\alpha=1}^{N-1} \phi^{\alpha\beta\gamma} \sin(\pi\alpha/N) \tag{3.11}$$

and

$$\phi_{N-1}^{\cdot\beta\gamma} = \sum_{\alpha=1}^{N-1} (-1)^{\alpha}\, \phi^{\alpha\beta\gamma} \sin(\pi\alpha/N). \tag{3.12}$$

This calculation involves two operations per interior mesh point. As we must evaluate sums for three pairs of boundaries, we need six operations per interior point in all. Thus we may find the source charges for the potential ψ_{rst} without synthesizing the entire mesh.

The determination of boundary values of ψ is described in the next section. We note here that the process used produces boundary potentials in each boundary plane as double sine transforms in the plane. Thus we may find the double sine transforms of the equivalent charge layers directly. We use the symbol E to denote equivalent charges and employ the notation of Eqs. (3.9), (3.10) for the various transforms. Then the equivalent charges in the plane $r = 1$ are given by

$$E_1^{\cdot\beta\gamma} = w_1 \psi_0^{\cdot\beta\gamma} \tag{3.13}$$

and similar equations apply on the other boundaries.

We write the transforms in the planes $s = 1$, $s = N - 1$, $t = 1$, and $t = N - 1$ as $E_1^{\alpha\cdot\gamma}$, $E_{N-1}^{\alpha\cdot\gamma}$, $E_1^{\alpha\beta\cdot}$, $E_{N-1}^{\alpha\beta\cdot}$, respectively. The contribution of the equivalent charges to the triple sine transform of the charge is obviously

$$\begin{aligned} E^{\alpha\beta\gamma} = {} & \{E_1^{\cdot\beta\gamma} + (-1)^{\alpha} E_{N-1}^{\cdot\beta\gamma}\} \sin \frac{\pi\alpha}{N} \\ & + \{E_1^{\alpha\cdot\gamma} + (-1)^{\beta} E_{N-1}^{\alpha\cdot\gamma}\} \sin \frac{\pi\beta}{N} + \{E_1^{\alpha\beta\cdot} + (-1)^{\gamma} E_{N-1}^{\alpha\beta\cdot}\} \sin \frac{\pi\gamma}{N}. \end{aligned} \tag{3.14}$$

Thus each transform coefficient may be obtained at a cost of six operations. It is then very easy to calculate $\psi^{\alpha\beta\gamma}$ and add it to $\phi^{\alpha\beta\gamma}$ before the final synthesis. Only one full synthesis is required.

The Fourier transforms give a contribution $\sim 15N^3 \log_2 N$ to the operation count. The calculation of correction charges and conversion factors adds a fixed overhead per interior point, which is much smaller, but is not negligible. In view of the dependence of practical computation times on the details of the implementation, there is little purpose in going into detail here. The reader will find it more useful to examine the examples of Section 6.

4. Calculation of the Boundary Potential

4.1. *The Basic Convolution Procedure*

In two-dimensional problems we may calculate the boundary potential by a primitive convolution procedure. For a square mesh of side N we have about $4N$ boundary points, and the simplest procedure requires about $32N^2$ operations. This compares with the Fourier transform time for the main mesh only if the mesh is very small.

In three dimensions we have about $6N^2$ boundary points and the operation count becomes $72N^4$. Careful organization of the calculation may change the constant in this expression but not the variable factor. To avoid spending an excessive time on the boundary calculation we adapt Hockney's FFT based convolution process [9].

Hockney's procedure is to double the size of the mesh in each direction, introducing zero charge on the additional points. He works with periodic transforms on the extended mesh. Various expressions of the procedure are possible, and the discussion of Ref. [9] is in terms of complex transforms. This is not convenient in our application. We work instead in terms of sine and of cosine transforms over the original mesh. We will show later that this effectively reproduces Hockney's zero-extended mesh.

Consider for a moment the one-dimensional convolution

$$\psi_u = \sum_{r=0}^{N} Q_r g_{u-r} \tag{4.1}$$

where g_r is a Green's function. As g_r is an even function of r, we may substitute the expansion

$$g_r = \sum_{r=0}^{N} g^\alpha \cos(\pi r\alpha/N), \tag{4.2}$$

valid in the range $(-N, N)$. This leads to the expression

$$\psi_u = \sum_{\alpha=0}^{N} g^\alpha \sum_{r=0}^{N} Q_r \cos\frac{\pi(u-r)\alpha}{N}. \tag{4.3}$$

We decompose the cosines in the usual way to find that

$$\begin{aligned}\psi_u &= \sum_{\alpha=0}^{N} g^\alpha \left\{\cos\frac{\pi u\alpha}{N}\left(\sum_{r=0}^{N} Q_r \cos\frac{\pi r\alpha}{N}\right) + \sin\frac{\pi u\alpha}{N}\left(\sum_{r=0}^{N} Q_r \sin\frac{\pi r\alpha}{N}\right)\right\} \\ &= \sum_{\alpha=0}^{N} \{g^\alpha Q^\alpha(C)\}\cos\frac{\pi u\alpha}{N} + \sum_{\alpha=1}^{N-1} \{g^\alpha Q^\alpha(S)\}\sin\frac{\pi u\alpha}{N}\end{aligned} \tag{4.4}$$

say. Thus we express ψ_u as the sum of contributions arising from a sine and a cosine transformation. The data for the sine (cosine) transformation comes from multiplying a coefficient of the Green's function transform by a coefficient of the sine (cosine) transform of the charges. The indices r, u, α take only values within the ranges of validity of the various expansions, and we need no assumptions about the behavior of the potential outside the mesh.

The relation to Hockney's method emerges if we consider the behavior of the various terms in the range $(0, 2N)$. If we extend the charges to $(N+1, 2N)$ by the rule

$$Q_{N+r} = Q_{N-r}, \tag{4.5}$$

the periodic transform over the extended range has a zero sine part, and the cosine coefficients are just twice the coefficients $Q^\alpha(C)$. Similarly, if we extend according to the rule

$$Q_{N+r} = -Q_{N-r} \tag{4.6}$$

the periodic transform contains only sine terms, which are equal to $2Q^{\alpha}(S)$. If we average these two distributions we obtain a zero-extended distribution. The transforms $Q^{\alpha}(C)$, $Q^{\alpha}(S)$ are clearly the cosine and sine parts of the periodic transform of this distribution. When we extend our analysis to three dimensions we have essentially a restatement of Hockney's procedure.

This restatement is useful in that it breaks up the potential in the three-dimensional case into several components, each of which may be considered separately. Thus it is easier to see how to exploit the hollowness of our charge distribution. We must, however, take some care to establish a suitable notation for the various transforms.

In the one-dimensional case, we may transform our charges in two ways, and the two transforms make different contributions to the potential. In three dimensions we have two choices of transform in each direction, or eight choices in all. We denote the choices by adding three arguments to the symbol for a charge transform. These arguments take "values" C or S to indicate whether cosine or sine transforms are in use. Thus we write

$$Q^{\alpha\beta\gamma}(C, C, C) = \sum_{r,s,t=0}^{N} Q_{rst} \cos\frac{\pi r\alpha}{N} \cos\frac{\pi s\beta}{N} \cos\frac{\pi t\gamma}{N} \tag{4.7}$$

for the triple cosine transform of the charges on a cubical mesh. To obtain any other transform we change one or more of the arguments C to S, and the corresponding cosines to sines, in Eq. (4.7).

Each of the eight charge transforms generates its own contribution to ψ_{rst}. We denote the contribution from (for example) the charge transform $Q^{\alpha\beta\gamma}(C, C, C)$ by $\psi_{rst}(C, C, C)$, where

$$\psi_{rst}(C, C, C) = \sum_{\alpha,\beta,\gamma=0}^{N} \psi^{\alpha\beta\gamma}(C, C, C) \cos\frac{\pi r\alpha}{N} \cos\frac{\pi s\beta}{N} \cos\frac{\pi t\gamma}{N} \tag{4.8}$$

and

$$\psi^{\alpha\beta\gamma}(C, C, C) = g^{\alpha\beta\gamma} Q^{\alpha\beta\gamma}(C, C, C). \tag{4.9}$$

We obtain other contributions by changing arguments C to S and corresponding cosines to sines in these equations.

It is important to note that we use the notation $Q^{\alpha\beta\gamma}(C, C, C)$ and so on to denote different triple transforms of one charge distribution Q_{rst}, but we use $\psi_{rst}(C, C, C)$, $\psi^{\alpha\beta\gamma}(C, C, C)$, and so on for the various contributions to the potential. Thus

$$\begin{aligned}\psi_{rst} = {} & \psi_{rst}(C, C, C) + \psi_{rst}(C, C, S) + \psi_{rst}(C, S, C) + \psi_{rst}(S, C, C) \\ & + \psi_{rst}(S, S, C) + \psi_{rst}(S, C, S) + \psi_{rst}(C, S, S) + \psi_{rst}(S, S, S)\end{aligned} \tag{4.10}$$

and there is no simple relationship between the terms on the right of Eq. (4.10).

The analysis above could be applied to any finite distribution of source charges. The coefficients generated would then all be generated at some stage by Hockney's process. In our case, however, the charge distribution is hollow. In Section 4.2 we

discuss the simplifications this introduces. In Sections 4.3 and 4.4 we consider the storage requirements and operation count for the boundary calculation.

4.2. *Convolution for a Hollow Charge Distribution*

To assist in visualizing the mesh, we regard r as the vertical coordinate of a mesh point, and s, t as the North and East coordinates, respectively. The same language may be applied to the transformed mesh and the indices α, β, and γ, even though the values of α, β, γ are not usually in their natural order. Fig. 1 is a sketch of the transformed mesh.

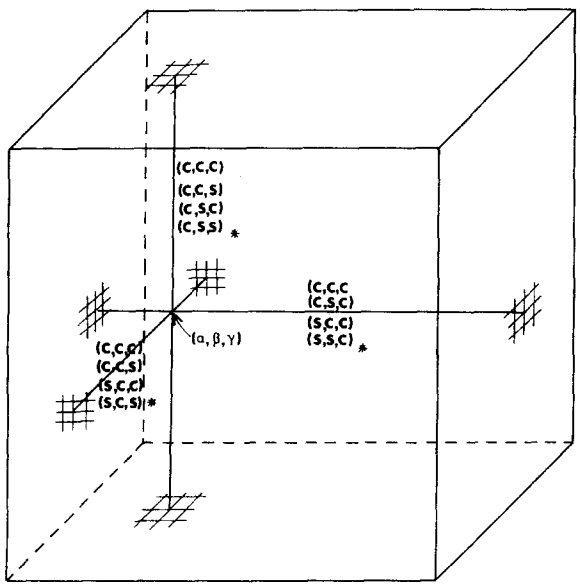

FIG. 1. The mesh in transform space. The point (α, β, γ) interacts only with its projections in the boundary planes. The perpendiculars to the boundaries are marked with the parameters (C, C, C), etc. of the charge transforms involved on these boundaries. Those marked $*$ are entirely parallel contributions, and are calculated from Eqs. (4.19), (4.20) and their counterparts on other boundaries, rather than in the main scan.

We consider first the charge transform $Q^{\alpha\beta\gamma}(C, C, C)$. This may be calculated from the double cosine transforms of charges in the boundary planes. We denote the transforms in the horizontal planes $r = 0$, $r = N$ by $Q_0^{\cdot\beta\gamma}(C, C)$ and $Q_N^{\cdot\beta\gamma}(C, C)$, respectively. We use $Q_0^{\alpha\cdot\gamma}(C, C)$, $Q_N^{\alpha\cdot\gamma}(C, C)$ for transforms in the South and North boundaries, and $Q_0^{\alpha\beta\cdot}(C, C)$, $Q_N^{\alpha\beta\cdot}(C, C)$ in the West and East boundaries. This is an obvious adaption of the notation for triple transforms.

To find the contribution of the horizontal boundaries to $Q^{\alpha\beta\gamma}(C, C, C)$ we simply perform the summation over r in Eq. (4.7), neglecting charges on other boundaries for the moment.

We obtain a contribution

$$Q_0^{\cdot\beta\gamma}(C, C) + (-1)^{\alpha} Q_N^{\cdot\beta\gamma}(C, C). \tag{4.11}$$

We proceed similarly for the other boundaries to obtain

$$\begin{aligned} Q^{\alpha\beta\gamma}(C, C, C) = &\{Q_0^{\cdot\beta\gamma} + (-1)^{\alpha} Q_N^{\cdot\beta\gamma}(C, C)\} \\ &+ \{Q_0^{\alpha\cdot\gamma} + (-1)^{\beta} Q_N^{\alpha\cdot\gamma}(C, C)\} \\ &+ \{Q_0^{\alpha\beta\cdot} + (-1)^{\gamma} Q_N^{\alpha\beta\cdot}(C, C)\}. \end{aligned} \tag{4.12}$$

We note in passing that we must adjust the edge and corner charges before evaluating this expression. Otherwise edge charges are counted twice and corner charges three times.

To obtain $\psi^{\alpha\beta\gamma}(C, C, C)$, we need only multiply Eq. (4.12) by $g^{\alpha\beta\gamma}$. We must then evaluate $\psi_0^{\cdot\beta\gamma}(C, C)$, $\psi_N^{\cdot\beta\gamma}(C, C)$, and the other double cosine transforms required. For the horizontal boundaries, the standard inversion formula reduces to

$$\psi_0^{\cdot\beta\gamma}(C, C) = (2/N) \sum_{\alpha=0}^{N}{}' \psi^{\alpha\beta\gamma}(C, C, C), \tag{4.13}$$

$$\psi_N^{\cdot\beta\gamma}(C, C) = (2/N) \sum_{\alpha=0}^{N}{}' (-1)^{\alpha} \psi^{\alpha\beta\gamma}(C, C, C), \tag{4.14}$$

where as usual the prime attached to $\sum$ shows that the contributions of the terms for $\alpha = 0$, $\alpha = N$ are halved. Similar sums over β and γ give the contributions on the vertical boundaries.

We do not divide terms like $\psi_0^{\cdot\beta\gamma}(C, C)$ into contributions from parallel and perpendicular boundaries. It is possible to construct procedures using such divisions, but we lose the advantage of dealing with a single function $\psi^{\alpha\beta\gamma}(C, C, C)$, and actually perform more operations.

The other contributions to the potential may be obtained in a similar way. We take $Q^{\alpha\beta\gamma}(C, C, S)$ as being typical of triple transforms involving sine transformation in one direction of the three. Clearly the East and West boundaries make no contribution to this transform, and the expression corresponding to Eq. (4.12) is

$$\begin{aligned} Q^{\alpha\beta\gamma}(C, C, S) = &\{Q_0^{\cdot\beta\gamma}(C, S) + (-1)^{\alpha} Q_N^{\cdot\beta\gamma}(C, S)\} \\ &+ \{Q_0^{\alpha\cdot\gamma}(C, S) + (-1)^{\beta} Q_N^{\cdot\beta\gamma}(C, S)\}. \end{aligned} \tag{4.15}$$

The rest of the procedure is as above, with the exception that we need not calculate any contributions on the East and West boundaries. Once again, we do not gain by splitting the contributions into parallel and perpendicular terms. We may permute the order of the arguments (C, C, S) to obtain all the boundary potential terms involving sine transformation in one direction.

The calculation of these terms may be interleaved with that of the double cosine terms, so that we do not introduce additional scans of the Green's function.

For the charge transform $Q^{\alpha\beta\gamma}(C, S, S)$, the form corresponding to Eq. (4.12) is

$$Q^{\alpha\beta\gamma}(C, S, S) = Q_0^{\cdot\beta\gamma}(S, S) + (-1)^\alpha Q_N^{\cdot\beta\gamma}(S, S). \tag{4.16}$$

Potential contributions must be calculated on the horizontal boundaries. From Eq. (4.16) we deduce that

$$\psi^{\alpha\beta\gamma}(C, S, S) = g^{\alpha\beta\gamma}\{Q_0^{\cdot\beta\gamma}(S, S) + (-1)^\alpha Q_N^{\cdot\beta\gamma}(S, S)\} \tag{4.17}$$

so, for example,

$$\psi_0^{\cdot\beta\gamma}(S, S) = \frac{2}{N}\left\{Q_0^{\cdot\beta\gamma}(S, S)\sum_{\alpha=0}^{N}{}' g^{\alpha\beta\gamma} + Q_N^{\cdot\beta\gamma}(S, S)\sum_{\alpha=0}^{N}{}'(-1)^\alpha g^{\alpha\beta\gamma}\right\}. \tag{4.18}$$

$(2/N)\sum_{\alpha=0}^{N}{}' g^{\alpha\beta\gamma}$ is the double cosine transform of g_{0st}, and $(2/N)\sum_{\alpha=0}^{N}{}'(-1)^\alpha g^{\alpha\beta\gamma}$ is that of g_{Nst}. Thus with the obvious notation, we may write Eq. (4.18) as

$$\psi_0^{\cdot\beta\gamma}(S, S) = g_0^{\cdot\beta\gamma}Q_0^{\cdot\beta\gamma}(S, S) + g_N^{\cdot\beta\gamma}Q_N^{\cdot\beta\gamma}(S, S). \tag{4.19}$$

Similarly

$$\psi_N^{\cdot\beta\gamma}(S, S) = g_N^{\cdot\beta\gamma}Q_0^{\cdot\beta\gamma}(S, S) + g_0^{\cdot\beta\gamma}Q_N^{\cdot\beta\gamma}(S, S). \tag{4.20}$$

We may save operations by using the expressions (4.19), (4.20). Similar expressions give the double sine terms on the vertical boundaries. Terms of this form involve parallel contributions only.

Finally, the triple sine transform of the hollow charge distribution is identically zero, and makes no contribution to the potential on any boundary.

The boundary calculation starts with double sine transforms of the boundary charges, together with edge and corner charges which are supplied separately. The final results are needed in the same form. The other transforms required in the course of the calculation could be obtained by inverting the sine transforms and cosine analyzing the results, at a cost of five operations per point and fold in each direction. These transformations must later be reversed.

While the cost is not prohibitive, a worthwhile saving follows if we express the process in terms of the discrete Hilbert transform. For a one-dimensional case, we define

$$x^\alpha(S) = \sum^{N-1} x_r \sin(\pi r\alpha/N) \tag{4.21}$$

$$x_r = \frac{2}{N}\sum_{\alpha=1}^{N-1} x^\alpha(S) \sin(\pi r\alpha/N) \tag{4.22}$$

for $r \neq 0, N$. The values of x_0, x_N are available separately. The cosine transform of the x_r's is

$$x^{\epsilon}(C) = \sum_{r=0}^{N} x_r \cos \frac{\pi r \xi}{N}$$

$$= x_0 + (-1)^{\epsilon} x_N + \sum_{\alpha=1}^{N-1} x^{\alpha}(S) \sum_{r=1}^{N-1} \sin \frac{\pi r \alpha}{N} \cos \frac{\pi r \xi}{N} \tag{4.23}$$

which we may reduce to

$$x^{\epsilon}(C) = x_0 + (-1)^{\epsilon} x_N + \sum_{\alpha=1}^{N-1} \{1 - (-1)^{\alpha+\epsilon}\} \frac{x^{\alpha}(S) \sin(\pi\alpha/N)}{\cos(\pi\xi/N) - \cos(\pi\alpha/N)}. \tag{4.24}$$

We obtain a similar Hilbert transform on changing from the cosine to the sine transform.

Although the discrete Hilbert transform does not look like a Fourier transform, we may perform similar folding operations on it, as in Ref. [11]. The operation count has leading term $3N \log_2 N$ as against $5N \log_2 N$ for synthesis and analysis. For short transforms we do not always realize this gain, but savings between 30% and 40% are normal.

4.3. *Storage Requirements for the Boundary Calculation*

The calculation must be carefully organized to avoid excessive demands for working space in core. The main part is best arranged as a single scan over horizontal planes in transform space. Nested within this we have a scan in the North direction, and at the next level a scan in the East direction. This inner scan evaluates several independent terms, and may be divided into independent scans. The code may thus be reduced to a series of very simple loops to exploit compiler optimization and relevant features of the computer architecture.

In scanning any horizontal plane (in transform space) we access every point of the horizontal boundaries. However, we need only those transform coefficients on the vertical boundaries which belong to the plane we are processing. Data and results for other planes can be held on sequential files if necessary. Thus our main storage requirement is for the horizontal boundary planes, on which we have data and results for double cosine, cosine–sine, and sine–cosine transforms. The double sine transforms involve contributions from parallel boundaries only, and may be evaluated separately.

To provide for data and results for the two horizontal boundaries would require $12N^2$ store locations. We may halve this by exploiting the property of most FFT processes of grouping even results together, followed by the odd results. Ziegler's algorithms have this property, even though they do not produce the usual bit-reversed order. Equation (4.12) shows that we need only the sum of the charge terms from the two horizontal boundaries if α is even, and the difference if α is odd. Equations (4.13), (4.14) show that even values of α contribute to the sum of the potentials on the two boundaries, and odd values of α to the difference. Thus we start by holding the sums

in core, and change to holding the differences nearly half way through the outer scan. Charge differences and potential sums may be held on a sequential file if necessary.

To the figure of $6N^2$ locations for the horizontal boundaries, we must add a few locations to hold boundary lines and working space. The Green's function can be held on a sequential file, and only buffer space is required.

4.4. *Operation Counts for the Boundary Calculation*

The boundary calculation falls into the following parts.

(1) Hilbert transformation of the boundary planes to obtain the various transforms required, and back transformation to obtain the boundary potentials in double sine form. For one plane of correction charges we may generate the other transforms with three Hilbert transformations. The cost of back-transformation is the same so we have a total of 18 operations per boundary point and fold. This leads to a count of $108N^2 \log_2 N$ operations in all.

(2) The main scan over the mesh to evaluate all but the double sine contributions. The sums and differences on the right of Eqs. (4.12), (4.15) are calculated outside the inner loops. Thus at each mesh point we need 9 operations to generate potential coefficients, and the same number to accumulate boundary terms. The leading term in the operation count is thus $18N^3$.

(3) The parallel term contributions, such as those of Eqs. (4.19), (4.20). These require 3 operations per boundary point, or $18N^2$ operations in all.

The last term is not significant, so the leading term in the operation count is $(18N^3 + 108N^2 \log_2 N)$. For a $33 \times 33 \times 33$ mesh this amounts to 1.23×10^6 operations, or about 46% of the work for sine analysis and synthesis on the main mesh. Reference to Section 6 shows that, owing to the logical complexity of the boundary calculation, we do not quite achieve this ratio.

5. Properties and Determination of the Green's Functions

To calculate the Green's function appropriate to any particular discrete form of the Laplace operator, we expand the function in powers of $1/R$ at large distances from the source. This expansion provides boundary values for a solution of Poisson's equation in the region surrounding a unit source charge. Thus we may find the nearby values. The procedure has been applied in two- and three-dimensional cases. In three dimensions it is usually adequate to use a simple expansion for the Green's function at a distance of 16 mesh intervals from the source.

For the five and nine point operators in two dimensions, we may compare with Buneman's analytic solutions [2, 3]. The agreement is excellent, and deviations from the logarithmic law are in accordance with his values. For the three-dimensional case, Figs. 2 to 4 show the deviations from a Newtonian potential for Green's functions $g_2(r, s, t)$, $g_3(r, s, t)$. These are inverse to discrete Laplace operators $\mathscr{L}_2$, $\mathscr{L}_3$, having

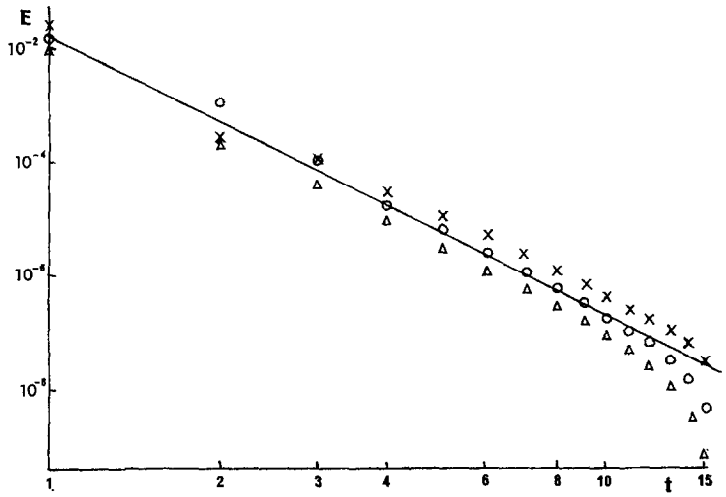

FIG. 2. Second-order formula on a symmetric mesh. E is the deviation from a Newtonian potential, t the number of mesh intervals from the source. $\times$ denotes points on the line $r = s = 0$, $\circ$ on $r = 0$, $s = t$, and $\triangle$ on $r = s = t$. The deviations should be compared with $g_2(0, 0, 0) \approx 1.9$.

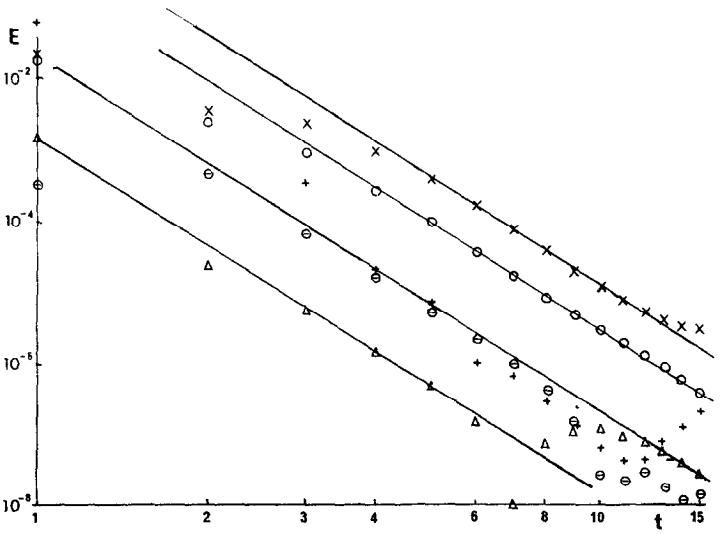

FIG. 3. Second-order formula on a nonsymmetric mesh. $\times$, $\circ$, $\triangle$ are as in Fig. 2, $+$ denotes points on the line $s = t = 0$ and $\ominus$ on the line $r = s$, $t = 0$. For the last two cases, the mesh index should be taken as s rather than t. $g_2(0, 0, 0) \approx 2$ for this formula.

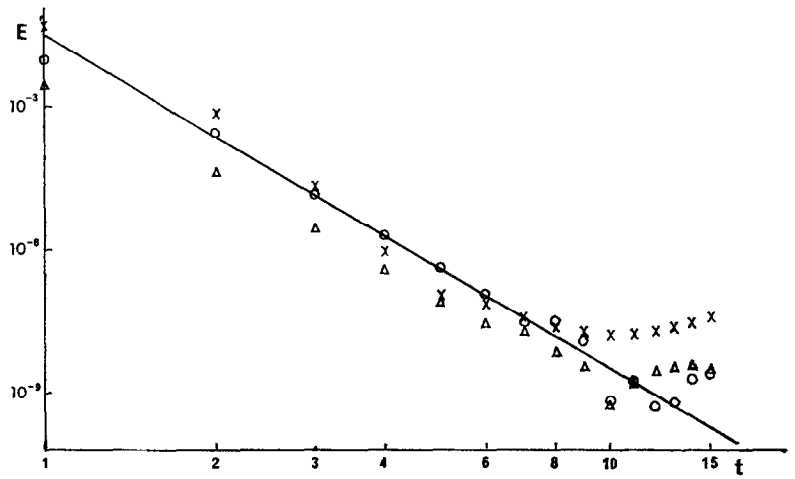

FIG. 4. Third-order formula on a symmetric mesh with $g_3(0, 0, Q) \approx 1.8$. Symbols have the meanings of Fig. 2.

fourth and sixth difference accuracy, respectively. Details of the error behavior are discussed in Appendix B for two- and three-dimensional cases.

To construct a distant expansion for the inverse of (say) the three-dimensional operator $\mathscr{L}_1$ of Eq. (3.2), we note that

$$\mathscr{L}_1(1/R) = O(R^{-5}). \tag{5.1}$$

In two dimensions we would operate on $\log_e R$ instead. We calculate the terms of order R^{-5} on the right-hand side of Eq. (5.1), and then find empirically a function $f(r, s, t)$ of order R^{-3} such that the leading terms in $\mathscr{L}_1\{f(r, s, t)\}$ and $\mathscr{L}_1\{R^{-1}\}$ agree. Thus

$$\mathscr{L}_1\{R^{-1} - f(r, s, t)\} = O(R^{-7}). \tag{5.2}$$

We may repeat this procedure to find the terms of order R^{-5}, R^{-7} and so on in the inversion of $\mathscr{L}_1$. The procedure for $\mathscr{L}_2$, $\mathscr{L}_3$ is essentially the same. We terminate the expansion at a convenient point and scale it to give the correct total flux across the boundary. Expansions for the various Green's functions used in three dimensions are listed in Appendix B.

It should be noted that the more accurate forms of the discrete Laplace operator may have implications for the scheme used to assign charges to mesh points. For example, as shown in Appendix A, the second-order discrete form for Eq. (2.1) may be written

$$\mathscr{L}_2\phi_{rst} = -\{1 + \tfrac{1}{12}(\delta_1^2 + \delta_2^2 + \delta_3^2)\}\, q_{rst}\,. \tag{5.3}$$

The difference terms on the right of Eq. (5.3) imply that the source appropriate to $\mathscr{L}_2$ is a monopole, together with three discrete quadrupoles.

Use of such a "molecule" of source charges would be most inconvenient in the boundary calculations of Section 4. Therefore, we operate on Eq. (5.3) with the operator

$$\mathscr{C} = 1 - \tfrac{1}{12}(\delta_1^2 + \delta_2^2 + \delta_3^2) \tag{5.4}$$

and calculate $\mathscr{C}g_2$. To the necessary accuracy this arises from a single source charge. In addition it also satisfies the discrete Laplace equation away from the source, and so its distant behavior is given by an expansion obtained as above. We may operate on the potential with $\mathscr{C}^{-1}$ to recover the correct Green's function g_2. This is essential to obtain the full accuracy of which the operator is capable, and has been done for the error estimates shown.

An alternative procedure is to operate on the source charges before solving for the potential. Thus to produce a monopole potential field as accurately as $\mathscr{L}_2$ allows, we need a charge $\frac{1}{2}q$ at the source (r, s, t), say, and charges $\frac{1}{12}q$ at the points $(r \pm 1, s, t)$, $(r, s \pm 1, t)$, and $(r, s, t \pm 1)$. With simple charge assignment schemes there may be little to choose between operating on the charges and on the potentials. Sophisticated schemes may possibly gain from incorporating the first procedure. It should be noted that one of these procedures is essential for the operator $\mathscr{L}_2$ if the mesh has unequal intervals. If the intervals are equal in all three directions, we see in Appendix A that the additional terms introduced in the potential are of order R^{-5}, and so are comparable with the error of the Green's function. For $\mathscr{L}_3$, a more complex charge molecule or potential reduction is needed. The details are given in Appendix A.

6. Performance of the Method

The procedure has been implemented on the CDC 7600 computer in the UMRCC system in Manchester. Most of the code is written in Fortran to the ANSI standard. The main exceptions are the mass storage routines and those which organize transfers between the large core (LCM) and small core (SCM) memories of the 7600.

The program has been compiled under the FTN 4.4 compiler at optimization level 2. This makes effective use of the machine's architecture when coding simple loops, and produces code of the quality we expect from an expert human programmer. The inner loops of the fast Fourier transform routines are sufficiently simple for this purpose. The other important routines, performing the screening charge and potential supplementation and the boundary calculation, have been divided into short parallel loops, within the conventions of ANSI Fortran. An experiment in recoding these loops in COMPASS gave small gains of random sign. Thus the computation times given in Table I are likely to be a realistic reflection of the costs of the various parts of the process.

Table I gives details of the reported CPU times for meshes of sizes $33 \times 33 \times 33$ and $65 \times 65 \times 65$ points. The smaller mesh fits into the LCM of the machine, but the larger has to be segmented and stored in mass storage records on a random access file. The solution time for the smaller mesh is about 2 seconds, and that for the larger

TABLE I

Computation Times in Seconds for the Major Divisions of the Calculation[a]

	$33 \times 33 \times 33$	$65 \times 65 \times 65$
FFT's on entire mesh	1.04	9.30
LCM/SCM block transfers	0.12	1.24
Mass store transfers	0	3.27
Screening charges/potential supplements:		
Operator $\mathscr{L}_1$	0.27	1.96
$\mathscr{L}_2$	0.43	3.77
$\mathscr{L}_3$	0.50	4.18
Boundary calculation	0.60	3.72
General organization	0.05	.30

[a] The times given are CPU times returned by the user-callable system monitoring routine SECOND.

between 20 and 22 seconds. The more accurate discrete Laplace operators $\mathscr{L}_2$, $\mathscr{L}_3$ require additional work in this implementation, as edge and corner terms for the screening and equivalent charge calculations are accumulated independently of the other terms. The costs could be reduced by working in terms of the boundary adjacent potentials, but additional core storage would be required.

The numerical accuracy of the program and method were checked by primitive convolution routines working with randomly chosen charges for small meshes, and with sparse charge distributions for large meshes. The deviations between the two potentials thus obtained were typically of order 10^{-7}.

APPENDIX A: Fourth and Sixth Difference Approximations to the Laplace Operator

The sixth difference approximation to Eq. (2.1) is

$$\begin{aligned} -q_{rst} = \{&(w_1\delta_1^2 + w_2\delta_2^2 + w_3\delta_3^2) \\ &- \tfrac{1}{12}(w_1\delta_1^4 + w_2\delta_2^4 + w_3\delta_3^4) \\ &+ (1/90)(w_1\delta_1^6 + w_2\delta_2^6 + w_3\delta_3^6)\}\phi_{rst}\,. \end{aligned} \tag{A1}$$

We rewrite the fourth difference terms as

$$\begin{aligned} -\tfrac{1}{12}\{&(\delta_1^2 + \delta_2^2 + \delta_3^2)(w_1\delta_1^2 + w_2\delta_2^2 + w_3\delta_3^2) \\ &- (w_2 + w_3)\,\delta_2^2\delta_3^2 - (w_3 + w_1)\,\delta_3^2\delta_1^2 \\ &- (w_1 + w_2)\,\delta_1^2\delta_2^2\}\phi_{rst}\,, \end{aligned} \tag{A2}$$

substitute for $(w_1\delta_1^2 + w_2\delta_2^2 + w_3\delta_3^2)\phi_{rst}$ from Eq. (A1) and drop eighth-order differences. On substituting back into Eq. (A1) and rearranging, we find that

$$\begin{aligned}
-\{1 + \tfrac{1}{12}(\delta_1^2 + \delta_2^2 + \delta_3^2)\}q_{rst} \\
&= \{w_1\delta_1^2[1 + \tfrac{1}{12}(\delta_2^2 + \delta_3^2)] + w_2\delta_2^2[1 + \tfrac{1}{12}(\delta_3^2 + \delta_1^2)] \\
&\quad + w_3\delta_3^2[1 + \tfrac{1}{12}(\delta_1^2 + \delta_2^2)]\}\phi_{rst} \\
&\quad + \{(1/90)(w_1\delta_1^6 + w_2\delta_2^6 + w_3\delta_3^6) \\
&\quad - (1/144)(\delta_1^2 + \delta_2^2 + \delta_3^2)(w_1\delta_1^4 + w_2\delta_2^4 + w_3\delta_3^4)\}\phi_{rst}\,. \qquad \text{(A3)}
\end{aligned}$$

Dropping the sixth difference terms leaves a three-dimensional form of the well-known "stencil" [6, 13]. The second-order approximation to the Poisson equation is therefore

$$\begin{aligned}
\mathscr{L}_2\phi_{rst} &= \{w_1\delta_1^2[1 + \tfrac{1}{12}(\delta_2^2 + \delta_3^2)] + w_2\delta_2^2[1 + \tfrac{1}{12}(\delta_3^2 + \delta_1^2)] \\
&\quad + w_3\delta_3^2[1 + \tfrac{1}{12}(\delta_1^2 + \delta_2^2)]\}\phi_{rst} \\
&= -\{1 + \tfrac{1}{12}(\delta_1^2 + \delta_2^2 + \delta_3^2)\}q_{rst}\,. \qquad \text{(A4)}
\end{aligned}$$

In the symmetric case of Eq. (2.6) we may reduce the sixth difference terms to a more tractable form. We drop the suffices on h_i, w_i, but refrain from substituting for w_i from Eq. (2.6). To do so would obscure the relationship of our equations to those above.

The sixth difference terms on the right of Eq. (A3) may be rearranged to give the expression

$$\begin{aligned}
w\{(1/30)\,\delta_1^2\delta_2^2\delta_3^2 + (7/720)(\delta_1^4 + \delta_2^4 + \delta_3^4)(\delta_1^2 + \delta_2^2 + \delta_3^2) \\
- (1/180)(\delta_1^2 + \delta_2^2 + \delta_3^2)^3\}\phi_{rst}\,. \qquad \text{(A5)}
\end{aligned}$$

The second and third terms on the right may be expressed as differences of q_{rst} when we drop eighth-order differences of ϕ_{rst}. The operator $(\delta_1^4 + \delta_2^4 + \delta_3^4)$ may be rearranged, and ultimately we obtain

$$\begin{aligned}
\mathscr{L}_3\phi_{rst} &= w\{(\delta_1^2 + \delta_2^2 + \delta_3^2) + \tfrac{1}{6}(\delta_2^2\delta_3^2 + \delta_3^2\delta_1^2 + \delta_1^2\delta_2^2) \\
&\quad + (1/30)\,\delta_1^2\delta_2^2\delta_3^2\}\phi_{rst} = -\mathscr{C}'^{-1}q_{rst} \qquad \text{(A6)}
\end{aligned}$$

where

$$\begin{aligned}
\mathscr{C}'^{-1}q_{rst} &= \{1 + \tfrac{1}{12}(\delta_1^2 + \delta_2^2 + \delta_3^2) \\
&\quad - (7/360)(\delta_2^2\delta_3^2 + \delta_3^2\delta_1^2 + \delta_1^2\delta_2^2) \\
&\quad + (1/240)(\delta_1^2 + \delta_2^2 + \delta_3^2)^3\}q_{rst}\,. \qquad \text{(A7)}
\end{aligned}$$

The two dimensional analog of Eq. (A4) is

$$\begin{aligned}
\mathscr{L}_2\phi_{rs} &= \{w_1\delta_1^2 + w_2\delta_2^2 + (1/24)\,\delta_1^2\delta_2^2\}\phi_{rs} \\
&= -\{1 + \tfrac{1}{12}(\delta_1^2 + \delta_2^2)\}q_{rs}\,. \qquad \text{(A8)}
\end{aligned}$$

There is no such analog to Eq. (A7).

The charge molecule defined by Eq. (A4) is discussed in Section 5. We note here that the full molecule need not be used for a symmetric mesh. The potential generated by the quadrupole terms is

$$-\tfrac{1}{12}(\delta_1^2+\delta_2^2+\delta_3^2)(A/R)$$
$$=(A/12R^3)\{(h_1^2+h_2^2+h_3^2)-(3/R^2)(h_1^4r^2+h_2^4s^2+h_3^4t^2)\}+O(R^{-5}). \tag{A9}$$

In the symmetric case we drop suffices on the h_i's and obtain a potential

$$\frac{Ah^2}{12R^3}\left\{3-\frac{3h^2}{R^2}(r^2+s^2+t^2)\right\}+O(R^{-5})=O(R^{-5}). \tag{A10}$$

This is comparable with the error term.

Similarly, for the molecule of Eq. (A7), the term in $(\delta_1^2+\delta_2^2+\delta_3^2)^3\,q_{rst}$ may be dropped. The other terms must be retained.

APPENDIX B: Properties of the Green's Functions

In this appendix we scale the geometrical distance by the factor $1/2(h_1^{-2}+h_2^{-2}+h_3^{-2})$, so that the distance variable is

$$R^2=\frac{r^2}{w_1}+\frac{s^2}{w_2}+\frac{t^2}{w_3}. \tag{B1}$$

The distant behavior of the Green's functions $g_1(r,s,t)$, $g_2(r,s,t)$, $g_3(r,s,t)$ inverse to the operators $\mathscr{L}_1$, $\mathscr{L}_2$, $\mathscr{L}_3$ is given by the expressions

$$g_1(r,s,t)=A\left\{\frac{1}{R}-\frac{1}{8}\left(\frac{1}{w_1}+\frac{1}{w_2}+\frac{1}{w_3}\right)\frac{1}{R^3}\right.$$
$$\left.+\frac{5}{8}\left(\frac{r^4}{{w_1}^3}+\frac{s^4}{{w_2}^3}+\frac{t^4}{{w_3}^3}\right)\frac{1}{R^7}+O(R^{-5})\right\}, \tag{B2}$$

$$g_2(r,s,t)=A\left\{\frac{1}{R}+\left[\frac{1}{4}\left(\frac{1}{{w_1}^2}+\frac{1}{{w_2}^2}+\frac{1}{{w_3}^2}\right)\right.\right.$$
$$\left.-\frac{1}{16}\left(\frac{1}{w_1}+\frac{1}{w_2}+\frac{1}{w_3}\right)^2\right]\frac{1}{R^5}$$
$$+\left[\frac{15}{32}\left(\frac{1}{w_1}+\frac{1}{w_2}+\frac{1}{w_3}\right)\left(\frac{r^2}{{w_1}^2}+\frac{s^2}{{w_2}^2}+\frac{t^2}{{w_3}^2}\right)\right.$$
$$\left.-\frac{15}{8}\left(\frac{r^2}{{w_1}^3}+\frac{s^2}{{w_2}^3}+\frac{t^2}{{w_3}^3}\right)\right]\frac{1}{R^7}$$
$$+\left[\frac{21}{4}\left(\frac{r^6}{{w_1}^5}+\frac{s^6}{{w_2}^5}+\frac{t^6}{{w_3}^5}\right)-\frac{105}{32}\right.$$
$$\left.\left.\times\left(\frac{r^4}{{w_1}^3}+\frac{s^4}{{w_2}^3}+\frac{t^4}{{w_3}^3}\right)\left(\frac{r^2}{{w_1}^2}+\frac{s^2}{{w_2}^2}+\frac{t^2}{{w_3}^2}\right)\right]\frac{1}{R^{11}}\right.$$
$$\left.+O(R^{-7}),\right\} \tag{B3}$$

and

$$g_3(r, s, t) = (A/R) + O(R^{-7}). \tag{B4}$$

The details of terms on the right of Eq. (B4) are not of interest, as the numerical values are small.

The leading terms in the deviations from the Newtonian potential are of order R^{-3}, R^{-5}, and R^{-7}, respectively. That for the function $g_1(r, s, t)$ cannot be considered satisfactory. Examples of deviations for the other formulas are shown in Figs. 2 to 4.

The Green's function we can use for a particular discrete operator is not, in fact, unique. Any harmonic, or solution of the discrete Laplace equation, may be added, and the mixture of harmonics actually present is determined by the expression used on the boundary. Most of these harmonics increase towards the boundary. The consequences are apparent in Fig. 4 for the function g_3. The straight line in this logarithmic diagram has index -7, and shows the expected behavior of deviations from a Newtonian potential. (The straight lines in this and other plots are intended as guides, and are not fits to any particular set of points.)

An interesting anomaly appears on inspecting Figs. 2, 3 for the function g_2. Figure 3 shows the deviations for a nonsymmetric mesh with $h_1 = 2h_2 = 2h_3$. The straight lines have index -5. The errors are greatest on the line $r = s = 0$, and are roughly of the magnitude predicted by the expansion (B3). We would expect the other errors shown to be smaller, as the abscissa is the number of cells separating the point from the source, and geometrical distances are least on $r = s = 0$. In fact many of the errors are anomalously small. The boundary potentials here were determined using the term A/R only and the harmonics introduced by this have the effect of reducing the errors still further in some places.

On inspecting Fig. 2 for a symmetric mesh, all the errors are smaller than we expect from Eq. (B3). The reason appears to be that the function

$$f(r, s, t) = \frac{3}{R^5} - \frac{5}{w^2R^9}(r^4 + s^4 + t^4) \tag{B5}$$

is an approximate harmonic, satisfying

$$\mathscr{L}_2\{f(r, s, t)\} = O(R^{-9}). \tag{B6}$$

Use of a simple expression at the boundary leads to a multiple of this harmonic being added to the Green's function. The effect is to reduce the deviations everywhere.

In the two-dimensional case, Buneman [2], Table I, gives exact values for the potential near the source for the five point Laplace operator. These potentials were reproduced with deviations less than 2×10^{-8}. Buneman also gives a simple and stable rule for the diagonal values, and these agree satisfactorily. The numerical table obtained by the methods of this paper is known to deviate from Buneman's solution by about 10^{-4} at a distance of 64 mesh intervals from the source. This arises because only the logarithmic term was used in applying the boundary condition at this distance, and the next term is of this order there. The deviations from Buneman's values were observed to increase smoothly to the expected value along the diagonal.

For the nine point operator, comparison is less straightforward as Buneman's recurrence relation, Ref. [3], for values on the line $r = 0$ (or $s = 0$) is unstable. Exact comparison values are available near the source only, and are again reproduced with deviations of order 10^{-8}. Off the line $r = 0$, Buneman's numerical values are reproduced to their full accuracy.

APPENDIX C: Potential and Charge Calculation for Various Laplace Operators

The relation between the charge and potential transforms is given by Eq. (3.5), where $C^{\alpha\beta\gamma}$ is defined by Eq. (3.6) for the simple operator $\mathscr{L}_1$. For the operators $\mathscr{L}_2$, $\mathscr{L}_3$ we replace $C^{\alpha\beta\gamma}$ by $C_2^{\alpha\beta\gamma}$, $C_3^{\alpha\beta\gamma}$, respectively, where

$$C_2^{\alpha\beta\gamma} = C^{\alpha\beta\gamma} - \tfrac{1}{3}(w_2 + w_3)\left(1 - \cos\frac{\pi\beta}{N}\right)\left(1 - \cos\frac{\pi\gamma}{N}\right)$$
$$- \tfrac{1}{3}(w_3 + w_1)\left(1 - \cos\frac{\pi\gamma}{N}\right)\left(1 - \cos\frac{\pi\alpha}{N}\right)$$
$$- \tfrac{1}{3}(w_1 + w_2)\left(1 - \cos\frac{\pi\alpha}{N}\right)\left(1 - \cos\frac{\pi\beta}{N}\right) \tag{C1}$$

and

$$C_3^{\alpha\beta\gamma} = C_2^{\alpha\beta\gamma} + \frac{4}{15}w\left(1 - \cos\frac{\pi\alpha}{N}\right)\left(1 - \cos\frac{\pi\beta}{N}\right)\left(1 - \cos\frac{\pi\gamma}{N}\right). \tag{C2}$$

The calculation of screening charges and equivalent charges for the operator $\mathscr{L}_1$ is particularly simple. The operator links only seven mesh points and no screening charges are needed on the edges and corners of the mesh. Similarly, the equivalent charges contain no contribution from the edge and corner potentials.

The operators $\mathscr{L}_2$, $\mathscr{L}_3$ link 19 and 27 mesh points, respectively. Both require screening charges on the edges of the mesh and involve edge contributions to the equivalent charges. In addition the calculations at interior points of the boundary planes are more complicated. At a point in the plane $r = 0$ for the operator $\mathscr{L}_2$ we may write

$$Q_{0st} = -(\mathscr{L}_2\phi)_{0st}\,. \tag{C3}$$

The only nonzero potentials on the right of this equation are in the plane $r = 1$, so

$$Q_{0st} = -\{w_1 + \tfrac{1}{12}(w_1 + w_3)\,\delta_2^{\,2} + \tfrac{1}{12}(w_1 + w_2)\,\delta_3^{\,2}\}\,\phi_{1st}\,. \tag{C4}$$

On transforming in directions 2 and 3 this reduces to

$$Q_0^{\cdot\beta\gamma} = -D_2^{\cdot\beta\gamma}\phi_1^{\cdot\beta\gamma} \tag{C5}$$

where

$$D_2^{\beta\gamma} = w_1 - \tfrac{1}{6}(w_1 + w_2)\left(1 - \cos\frac{\pi\beta}{N}\right) - \tfrac{1}{6}(w_1 + w_3)\left(1 - \cos\frac{\pi\gamma}{N}\right). \tag{C6}$$

Similar relations apply on other boundaries. The equivalent charges follow if we simply change the sign in Eq. (C5). For the operator $\mathscr{L}_3$ a similar treatment gives Eq. (C5) with multiplier

$$D_3^{\beta\gamma} = D_2^{\beta\gamma} + \frac{2}{15}\, w\left(1 - \cos\frac{\pi\beta}{N}\right)\left(1 - \cos\frac{\pi\gamma}{N}\right). \tag{C7}$$

For the screening charges on, for example, the edge $r = s = 0$, Eq. (C4) reduces to

$$Q_{00t} = -\tfrac{1}{12}(w_1 + w_2)\,\phi_{11t} \tag{C8}$$

for the operator $\mathscr{L}_2$. The corresponding equation for $\mathscr{L}_3$ is

$$Q_{00t} = -w(\tfrac{1}{6} + (1/30)\,\delta_3{}^2)\,\phi_{11t} \tag{C9}$$

which reduces to a multiplication on sine transforming in direction 3. The relationship between E_{11t} and ψ_{00t} again follows by changing the sign in Eq. (C9).

Finally the screening charges at the corners are nonzero for the operator $\mathscr{L}_3$ only. In this case, as example,

$$Q_{000} = -(w/30)\,\phi_{111} \tag{C10}$$

and

$$E_{111} = (w/30)\,\psi_{000} \tag{C11}$$

Acknowledgments

I would like to thank Professor F. D. Kahn for his advice and encouragement in this work, and Professor O. Buneman for his valuable comments on an earlier version of this paper. An anonymous referee drew my attention to the apparent discrepancy between the errors in Figs. 2 and 3, which is discussed in Appendix B. It is a pleasure to acknowledge this contribution.

References

1. J. P. Boris and K. V. Roberts, *J. Computational Phys.* **4** (1969), 552.
2. O. Buneman, *J. Computational Phys.* **8** (1971), 500.
3. O. Buneman, *J. Computational Phys.* **11** (1973), 447.
4. B. L. Buzbee, F. W. Dorr, J. A. George, and G. H. Golub, *SIAM J. Numer. Anal.* **8** (1971), 722.
5. J. W. Cooley and J. W. Tukey, *Math. Comp.* **19** (1965), 297.
6. J. W. Eastwood and R. W. Hockney, *J. Computational Phys.* **16** (1974), 342.
7. K. von Hagenow and K. Lackner, "Proc. 7th Conference on Numerical Simulation of Plasmas," New York, 1975.

8. R. W. HOCKNEY, *Astrophys. J.* **150** (1967), 797.
9. R. W. HOCKNEY, *Methods Computational Phys.* **9** (1970), 135.
10. R. W. HOCKNEY AND D. R. K. BROWNRIGG, *Mon. Not. Roy. Astron. Soc.* **167** (1974), 361.
11. F. HOHL, *J. Computational Phys.* **9** (1972), 10.
12. R. A. JAMES, in preparation, (1976).
13. L. V. KANTOROVICH AND V. I. KRYLOV, "Approximate Methods of Higher Analysis," p. 185, Groningen, Noordhoff, 1958.
14. J. A. MARUHN, T. A. WELTON, AND C. Y. WONG, *J. Computational Phys.* **20** (1976), 326.
15. H. ZIEGLER, *IEEE Trans.* **AU-20** (1972), 353.